

# Use of the absolute phase in frequency modulated continuous wave plasma reflectometry

G. Cunningham

EURATOM/UKAEA Fusion Association, Culham Science Centre, Abingdon, Oxon OX14 3DB, United Kingdom

(Received 7 March 2008; accepted 6 July 2008; published online 4 August 2008)

In frequency modulated continuous wave reflectometry, used for density profile measurement in fusion plasmas, it is usual to measure the beat frequency between the launched wave and the reflected wave, and from this to calculate the position of the reflecting layer in the plasma. The absolute phase of the beat signal is usually neglected. The reason is that the phase shift between sweeps is usually comparable with or more than  $2\pi$ , leading to an ambiguity that is impossible to resolve. However, recent observations on the MAST tokamak have shown that, under quiet plasma conditions (this term has to be defined), the phase shift between sweeps is small compared with  $2\pi$  and the phase ambiguity can be readily resolved. The reflectometer signal is then being analyzed as an interferometer signal would normally be, and there is a substantial improvement in spatial resolution. The method is illustrated by application to small edge localized mode precursor and allows what is believed to be the first quantitative measurement of the displacement of the plasma boundary by such a precursor mode. The errors in both the absolute phase measurement and the more conventional frequency measurement are also estimated. © 2008 American Institute of Physics. [DOI: 10.1063/1.2964233]

## I. INTRODUCTION

The MAST frequency modulated continuous wave (FMCW) reflectometer is technically similar to that on ASDEX-U,<sup>1</sup> but has only three wavebands all located on the low field side of the tokamak. The general scheme is shown in Fig. 1. The three bands are *K* band (probing frequency  $f_p$  from 17 to 27 GHz), *Ka* band (from 26 to 40 GHz), and *U* band (from 39 to 54 GHz), and are polarized with the  $\vec{E}$  vector parallel to the toroidal field. Although the poloidal field in MAST can be up to half of the toroidal field, the reflected wave will still be dominated by the “ordinary mode” component. The system is normally operated by sweeping across the bands in 20  $\mu$ s and the detector signal is recorded at 50 MHz, with 8 bit resolution. However, for the work described here, it was swept with a reduced period of 2.5  $\mu$ s, at 3  $\mu$ s intervals. To achieve this it was necessary to reduce the frequency range, for example, the *Ka* band was operated only from 30 to 31.2 GHz.

Figure 2 shows the unprocessed signals from a succession of ten sweeps in the *Ka* band, and it is apparent that the phase shift between sweeps is fairly small. We refer to this situation as the “quiet plasma,” and several factors contribute to its attainment. Firstly, the plasma is in *H* mode, and the MAST *H* mode plasma typically has a high and steep density pedestal, with a scale length of about 2 cm. Such a steep gradient means that even substantial density fluctuations give a rather small variation in optical path. Secondly, use of a reduced sweep period reduces the movement of the reflecting layer between sweeps. Thirdly, there is a fairly low level of magnetohydrodynamic (MHD) activity, especially high frequency activity such as energetic particle modes.

Figure 3 shows the same signals as Fig. 2 over a longer time, and it is apparent that coherence between sweeps is maintained even while a MHD mode is growing (0.2514–0.2516 s). Measurement of this mode will be used to illustrate the benefit of absolute phase interpretation.

## II. ANALYSIS

In a reflectometer, the signal is produced by mixing a proportion of the outgoing wave with the wave reflected from the plasma, and Ginzburg,<sup>2</sup> Eq. (30.6), p. 351, has shown that, provided the permittivity changes slowly over a wavelength (the WKB approximation), the phase between these waves is given by

$$\phi(\omega) = \frac{2\omega}{c} \int_0^{z[\epsilon(\omega)=0]} n(\omega, z) dz - \frac{\pi}{2},$$

where  $\omega$  is the angular frequency of the wave,  $z$  is the distance in the direction of propagation,  $n(\omega, z)$  is the refractive index, and  $\epsilon$  is the permittivity,  $\epsilon = n^2$ . The upper limit of the integration  $z[\epsilon(\omega)=0]$  is the position of the “cut-off” density at which the wave is reflected. In FMCW reflectometry  $\omega$  is continually swept and by differentiating the above with respect to  $\omega$ , as Hubbard,<sup>3</sup> Eq. (2.13), p. 59, shows, the phase continually changes at a rate

$$\frac{d\phi}{d\omega} = 2 \int_0^{z[\epsilon(\omega)=0]} \frac{1}{v_g(\omega, z)} dz,$$

where  $v_g$  is the group velocity, see Ref. 2, Eq. (21.18), p. 232. Hence if the sweep rate is  $d\omega/dt$ , then

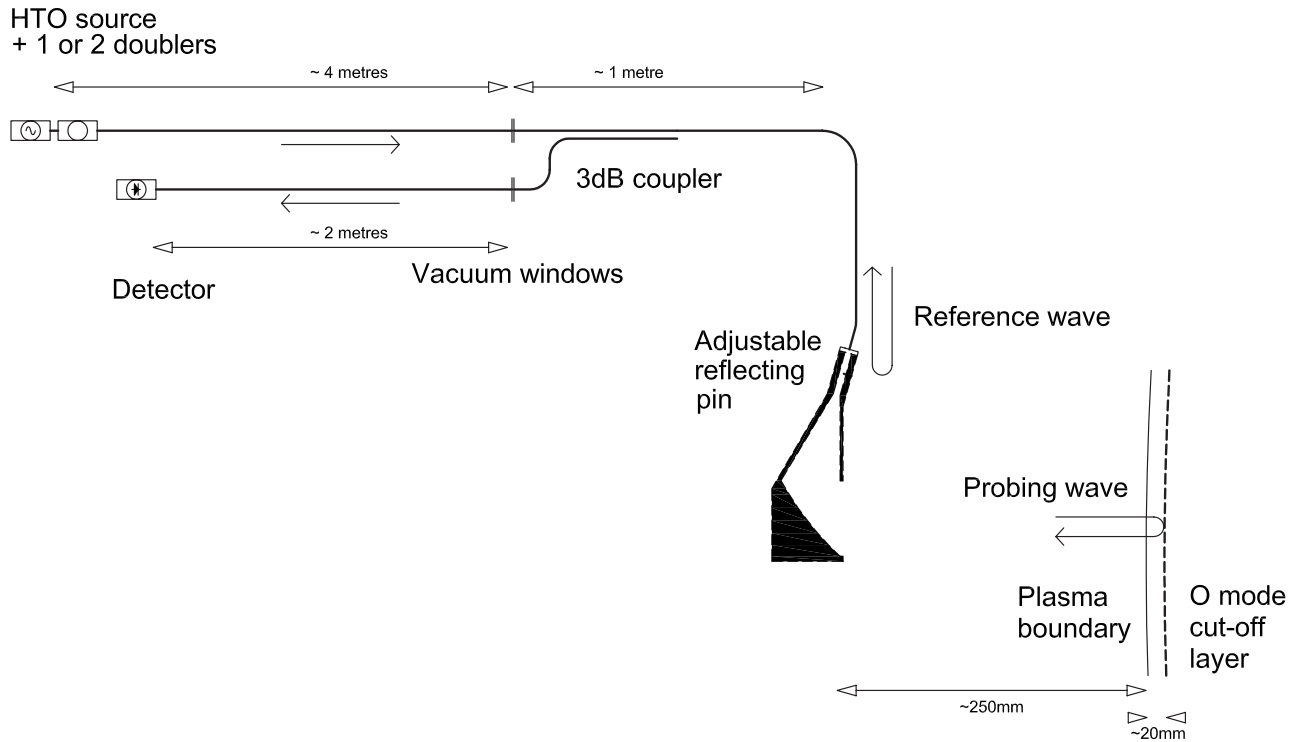


FIG. 1. General scheme of one waveband channel of the MAST reflectometer. Also shown is the approximate position of the plasma boundary and the reflecting layer for 30 GHz.

$$\frac{d\phi}{dt} = 2 \frac{d\omega}{dt} \int_0^{z[\epsilon(\omega)=0]} \frac{1}{v_g(\omega, z)} dz. \tag{1}$$

The continually changing phase is detected as a signal having frequency that is known as the beat frequency,  $f_b = (1/2\pi)(d\phi/dt)$ , which is subsequently measured as described below. Equation (1) is conveniently abbreviated by introducing the group delay, [Ref. 2, Eq. (30.11) p. 352],

$$\Delta t_g = 2 \int_0^{z[\epsilon(\omega)=0]} \frac{1}{v_g} dz, \tag{2}$$

giving

$$f_b = \Delta t_g \frac{df_p}{dt}. \tag{3}$$

We will also use the group path  $L_g = c\Delta t_g$ .

Signals such as those in Fig. 2 are analyzed using the digital complex demodulation (CDM) method, see Refs. 4–6. In this, the signal  $S$  is multiplied by a complex periodic signal  $R(t) = e^{i\omega_r t} = e^{i\phi_r(t)}$  where  $\omega_r$  is approximately the same frequency as the signal. The product is low-pass filtered, the phase extracted, and added to the initial estimate.

$$Y(t) = \text{lowpass}(RS),$$

$$\delta\phi(t) = \arctan[Y(t)],$$

$$\phi(t) = \phi_r(t) - \delta\phi(t).$$

The difference between  $\omega_r$  and the frequency of the signal must be less than the characteristic frequency of the low-pass filter, which can thus be considered as the capture range. When the sweep range is relatively narrow then the beat

frequency is sensibly constant so it is practicable to obtain the mean beat frequency and the absolute phase by making a straight line fit,  $\phi(t) = \phi_0 + 2\pi f_b t$ . Figure 4 shows the two quantities  $f_b$  and  $\phi_0$  over the same interval as Fig. 3.

### III. CONFIDENCE AND ERRORS

It is useful to check that  $\cos(\phi)$  is actually a good representation of the observed signal  $S$ , and this is readily achieved by calculating the correlation coefficient between  $S$  and  $\cos(\phi)$  for each sweep, see Fig. 4, upper trace. For the

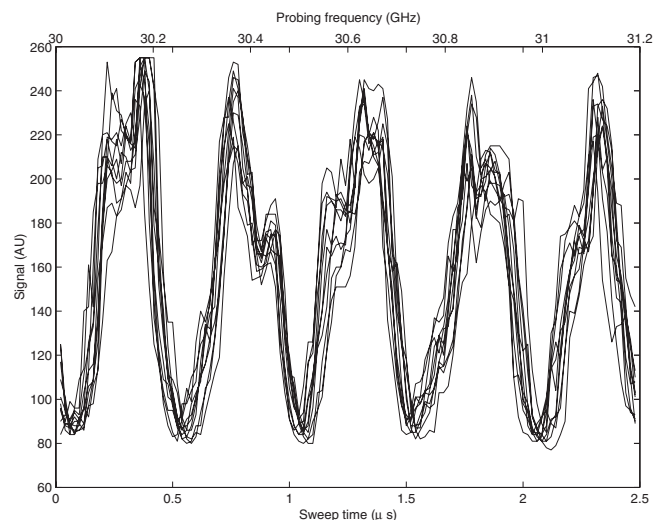


FIG. 2. Ten successive sweeps of unprocessed  $Ka$  band signal. The periodic signal is caused by sweeping of the source frequency. The fact that the signal is fairly coherent from sweep to sweep indicates that the plasma is “quiet” (see Sec. I).

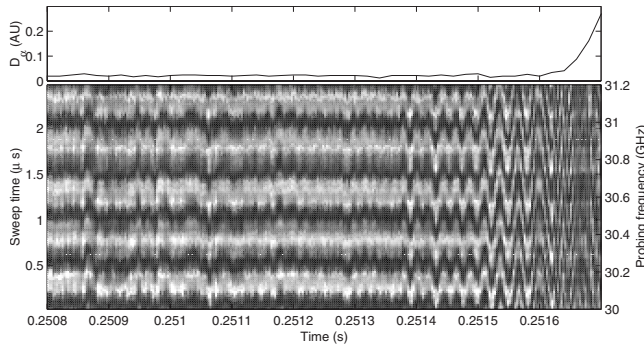


FIG. 3. Unprocessed  $K\alpha$  band signal over an extended period (1 ms, 333 sweeps, compared with the  $30 \mu\text{s}$ , 10 sweeps shown in Fig. 2). This is a “pseudocolor” plot, where the detector voltage is represented on a scale from black to white. Each sweep occupies a column of pixels, so that each row of pixels represents the signal phase for a particular probing frequency as a function of time.

signals considered here the correlation coefficient is more than 0.8 for all the signals prior to the edge localized mode<sup>7</sup> (ELM) (at 0.2516 s), so they are all included in subsequent analysis. This high correlation also implies that the noise level is fairly low so a linear analysis of the error propagation will be satisfactory. We also assume that there is a negligible incidence of phase jumps, and this is justified because in the data shown in Fig. 4, prior to 0.2516 s, there is only one occasion when  $\phi_0$  changes by more than  $\pi/2$  rad between sweeps.

It is not entirely obvious how the noise in the signal will propagate through the analysis of  $\phi_0$  and  $f_b$ , so we adopt the rather pedantic approach of generating a set of synthetic signals with statistical characteristics matching the observed signal and passing them through the same analysis procedure. The first step, however, is to characterize the noise in the signal. Noise may originate from phase noise in the microwave source, amplitude noise in the detector, and both amplitude and phase noise from fluctuations in the plasma. However, all of these are considered collectively in the amplitude direction only. Clearly, such a simple approach would not be adequate if the intent were to make a study of the statistical properties of plasma fluctuations, but since we only aim to estimate the errors in  $\phi_0$  and  $f_b$ , it is considered to be satisfactory. It should also be made clear that since the analysis is based on a particular set of data, the result will only be applicable to that set, and no general statement on the measurement error under different conditions can be made.

Since there is significant distortion in the signal waveform, the noise is estimated by comparing individual sweep measurements with an average over many sweeps. Systematic variation due to movement of the plasma is first removed by mapping from  $S(t)$  to  $S(\phi)$ . Figure 5 shows the set of signals, their mean, and the standard deviation of the residuals. The probability distribution function and the spectrum of the residuals are also calculated and shown. These statistics are then used to generate a set of 200 synthetic noise signals, which are added to the mean of the observed signals and passed through the CDM analysis. The resulting beat frequency has a standard deviation  $\sigma=13$  kHz (compared

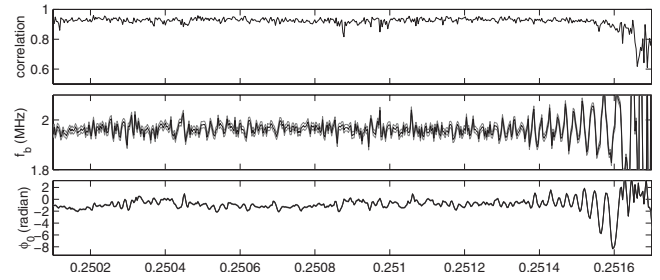


FIG. 4. Output of the CDM analysis of the signals in Fig. 3. The middle and lower traces also show lines one standard deviation above and below the direct result, although in the latter case this is too close to resolve by the eyes.

with a mean of about 2 MHz), and the absolute phase has  $\sigma=0.06$  rad, and these are shown in Fig. 4 although the latter is too small to be visible.

#### IV. DOPPLER EFFECT

Ginzburg,<sup>2</sup> Eq. (30.24), p. 358, showed that if the plasma varies over time but at a rate that is slow compared with the wave frequency, then the Doppler effect leads to a frequency shift in the reflected wave of

$$\Delta\omega = -\frac{2\omega}{c} \int_0^{z[\epsilon(\omega)=0]} \frac{\partial n}{\partial t} dz. \quad (4)$$

When the reflected wave is mixed with the outgoing wave, this shift results in a detected frequency, which can be written as

$$\Delta f_d = \frac{f_p}{c} \frac{dL_o}{dt}, \quad (5)$$

$L_o$  being the optical path.

The fact that the Doppler shift depends on the optical path while the beat frequency depends on the group path means that we cannot properly compare them without knowing the full profile. However, for the sake of discussion, we can make the simplifying assumption that the profile is moving rigidly back and forth as shown in Fig. 6, then the only path changes are in the vacuum region where  $\mu=1$  and  $\Delta L_g = \Delta L_o = \Delta L$ .

Let us also assume that  $L$  varies periodically,  $\Delta L = L_1 \cos(2\pi f_m t)$ , for example, due to a MHD mode, in which case modulation of the detected frequency will be dominated by the Doppler shift when

$$\begin{aligned} \Delta f_d > \Delta f_b &\Rightarrow \frac{f_p}{c} \frac{dL}{dt} > \frac{\Delta L}{c} \frac{df_p}{dt} \Rightarrow f_p L_1 2\pi f_m > L_1 \frac{df_p}{dt} \\ &\Rightarrow f_m > \frac{1}{2\pi f_p} \frac{df_p}{dt}, \end{aligned}$$

which in this case gives a transition frequency  $f_m \approx 3$  kHz. Since mode frequency in Fig. 4 is about 40 kHz, the modulation in the detected frequency is primarily due to the Doppler shift rather than variation in the group delay.

The absolute phase also suffers from the Doppler shift, but the transition frequency is much higher. In the absence of Doppler shift, the phase shift due to variation in  $L$  will be

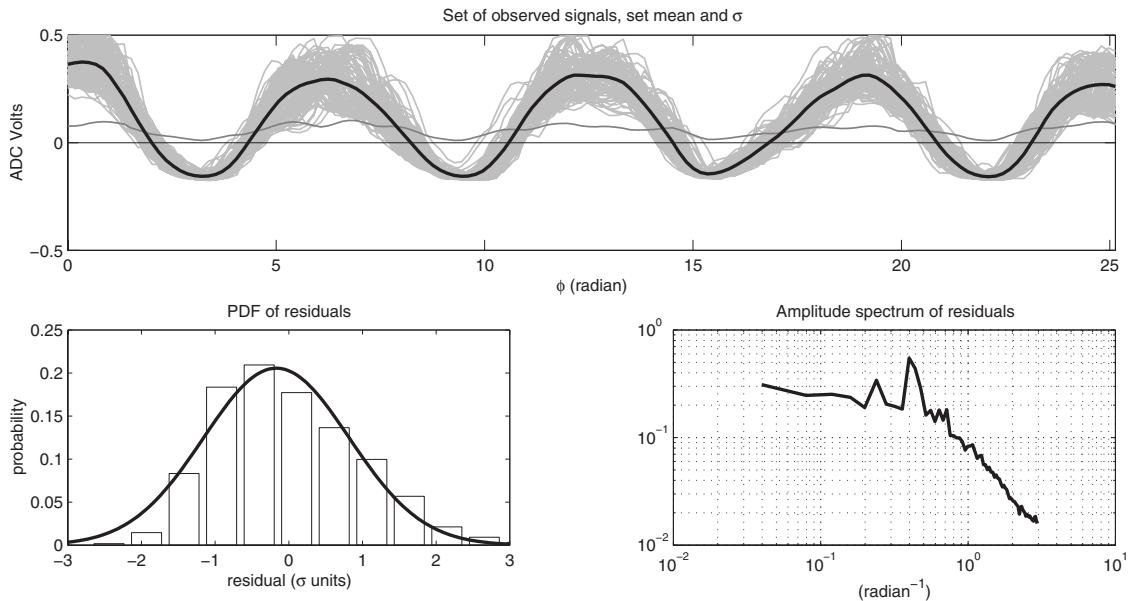


FIG. 5. Analysis of the errors in the *Ka* band signal.

$$\Delta\phi_z = 2\pi \frac{L_1}{\lambda} = 2\pi \frac{L_1 f_p}{c} \tag{6}$$

On the other hand the Doppler shift in the frequency of the return wave, Eq. (4), corresponds to a shift in wavelength of

$$\frac{\Delta\lambda}{\lambda} = \frac{1}{c} \frac{dL}{dt} = \frac{L_1 2\pi f_m}{c}$$

which in turn will cause a phase shift at the detector

$$\Delta\phi_d = 2\pi \frac{l}{\lambda} \frac{\Delta\lambda}{\lambda} = 2\pi \frac{l f_p}{c} \frac{L_1 2\pi f_m}{c}$$

where *l* is the distance traveled by the frequency shifted wave, that is, the distance from the reflecting layer to the detector (about 4 m in this case). The Doppler shift will dominate when

$$\Delta\phi_d > \Delta\phi_z \Rightarrow 2\pi \frac{l f_p}{c} \frac{L_1 2\pi f_m}{c} > 2\pi \frac{L_1 f_p}{c} \Rightarrow f_m > \frac{c}{2\pi l}$$

which in this case is about 12 MHz—well above the MHD mode frequency.

These approximate calculations are supported by the analysis of the experimental data of Fig. 4. In Fig. 7, second trace, the absolute phase signal  $\Delta\phi$  is converted to a displacement using Eq. (6). In the third trace the detected frequency is interpreted as a beat frequency in the conventional way. The variations are clearly much larger than indicated by the phase (note the expanded y axis), and during the MHD mode they are also  $\pi/2$  out of phase; however, if the detected signal is actually due to Doppler shift, this is exactly what we should expect. In the fourth trace the detected frequency is interpreted as a Doppler shift and converted to a velocity using Eq. (5), then converted to a displacement by integration with respect to time. It is clear that for short timescales, i.e., those of the MHD mode, this interpretation

is in agreement with the phase interpretation in both amplitude and phase; naturally, for longer timescales this interpretation gives a false result.

V. CONCLUSION

The ELM precursor mode seen here has a frequency of about 40 kHz and a growth time of about 0.2 ms. It reaches an amplitude of about 5 mm before the ELM enters its “explosive” phase and the  $D_\alpha$  signal starts to increase. Modes of this type have been observed before, both using fast interferometry<sup>8</sup> and fixed frequency reflectometry,<sup>9</sup> but this is believed to be the first quantitative measurement of the mode amplitude. Prior to onset of the mode there is more turbulent activity that has a generally  $1/f$  spectrum but with a distinct peak at about 50 kHz, which may indicate that the same mode is already present.

As mentioned at the beginning of the last section, the “amplitude” referred to here is the amplitude of a modulation in the group path length. Strictly speaking we cannot convert this to a physical path without measuring the whole profile and making an Abel inversion, but if we were to make the simplifying approximation that the profile is moving rigidly

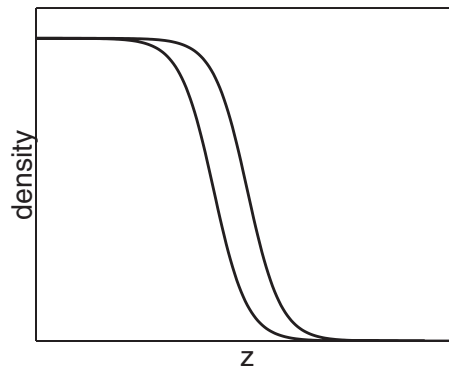


FIG. 6. Simplified representation of profile modulation.

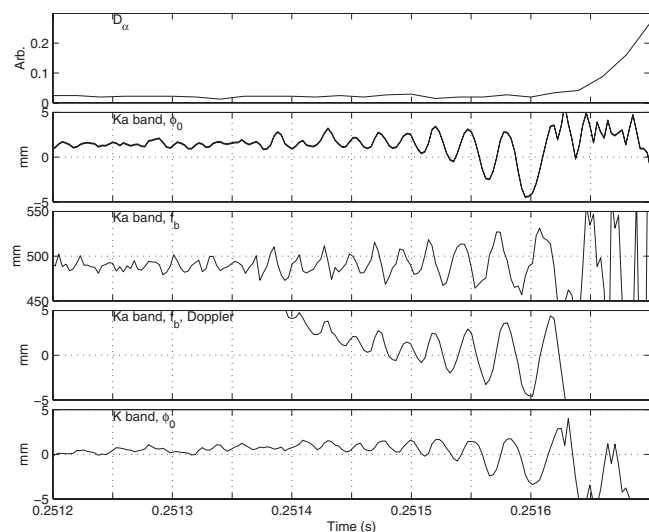


FIG. 7. (Top trace)  $D_\alpha$  signal. (Traces 2 and 3) Phase and beat frequency data from Fig. 4 converted to physical units. (Trace 4) Frequency data from Fig. 4 interpreted as a Doppler shift to give a velocity, then converted to a displacement by integrating with respect to time. (Bottom trace) As trace 2, but derived from the  $K$  band signal.

back and forth, then modulation in the group path could be equated to a physical displacement. Evidence that this approximation is reasonable comes from similar data recorded at the same time on the  $K$  band (22 GHz), Fig. 7, bottom trace, since the mode amplitude at this probing frequency is similar to the  $Ka$  band. It is also possible that such a small modulation might originate from contamination by  $X$  mode signal and modulation of that signal by magnetic field fluctuation. However, the  $H$  mode density profile in MAST is so steep that, even if the signal were entirely  $X$  mode, there would have to be a modulation of more than 10% in the total field to produce an effect of the magnitude seen; this possibility can therefore be discounted.

$O$  mode FMCW reflectometer signals observed during an inter-ELM period during a MAST  $H$  mode plasma discharge have been analyzed both using the conventional beat

frequency interpretation and by comparing the absolute phase in successive sweeps. It has been shown that the use of the absolute phase, when possible, gives much improved resolution in the measurement of small plasma displacements. Perhaps more important, it is also effectively immune to the Doppler effect so that interpretation is very much more straightforward.

## ACKNOWLEDGMENTS

The author is indebted to E. Doyle for discussions on the CDM method, and to S. Heuraux for pointing out the significance of the Doppler effect. The MAST reflectometer was built under a UKAEA-IST collaboration, particularly by A. Silva and L. Meneses of IST, Lisboa. This work was funded jointly by the United Kingdom Engineering and Physical Sciences Research Council and by the European Communities under the Contract of Association between EURATOM and UKAEA. The views and opinions expressed herein do not necessarily reflect those of the European Commission.

- <sup>1</sup>A. Silva, M. E. Manso, L. Cupido, M. Albrecht, F. Serra, P. Varela, J. Santos, S. Vergamota, F. Eusébio, J. Fernandes, T. Grossmann, A. Kallenbach, B. Kurzan, C. Loureiro, L. Meneses, I. Nunes, F. Silva, and W. Suttrop, *Rev. Sci. Instrum.* **67**, 4138 (1996).
- <sup>2</sup>V. L. Ginzburg, *The Propagation of Electromagnetic Waves in Plasmas* (Pergamon, New York, 1964).
- <sup>3</sup>A. E. Hubbard, "Measurement of electron density on JET by microwave reflectometry," Ph.D. thesis, Imperial College of Science and Technology, 1987.
- <sup>4</sup>D. Choi, E. Powers, R. Bengston, and G. Joyce, *Rev. Sci. Instrum.* **57**, 1989 (1986).
- <sup>5</sup>K. Kim, E. Doyle, T. Rhodes, W. Peebles, and C. Rettig, *Rev. Sci. Instrum.* **68**, 466 (1997).
- <sup>6</sup>J. P. S. Bizarro and A. C. Figueiredo, *Rev. Sci. Instrum.* **70**, 1030 (1999).
- <sup>7</sup>The ELM in a tokamak plasma is a brief period of intense activity localised at the plasma edge, and characteristic of the "high confinement" mode of operation. It can be identified by a rapid burst of deuterium Balmer  $\alpha$  light ( $D_\alpha$ ).
- <sup>8</sup>R. Scannell, A. Kirk, N. B. Ayed, P. G. Carolan, G. Cunningham, J. McCone, S. L. Prunty, and M. J. Walsh, *Plasma Phys. Controlled Fusion* **49**, 1431 (2007).
- <sup>9</sup>M. Manso, F. Sera, I. Nunes, J. Santos, A. Silva, W. Suttrop, P. Varela, and S. Vergamota, *Plasma Phys. Controlled Fusion* **40**, 747 (1998).